Exp. Anim. 68(4), 549–558, 2019

—Original—

Astragaloside IV reduces cardiomyocyte apoptosis in a murine model of coxsackievirus B3-induced viral myocarditis

Tianlong LIU[1)]*, Fan YANG[2)]*, Jing LIU[1)]*, Mingjie ZHANG[1)], Jianjun SUN[1)], Yunfeng XIAO[3)], Zhibin XIAO[3)], Haiyan NIU[2)], Ruilian MA[1)], Yi WANG[1)], Xiaolei LIU[3)] and Yu DONG[4)]

[1)]*Department of Pharmacy, Affiliated Hospital of Inner Mongolia Medical University, No. 1 Tongdao North Street, Huimin District, Hohhot 010059, P.R. China*
[2)]*Department of Service Center, Health committee of Inner Mongolia Autonomous Region, No. 63 Xinhua Street, Xincheng District, Hohhot 010055, P.R. China*
[3)]*Department of Pharmacology, Inner Mongolia Medical University, Jinshan Development Zone, Hohhot 010059, P.R. China*
[4)]*Department of Natural Medicinal Chemistry, College of Pharmacy, Inner Mongolia Medical University, Jinshan Development Zone, Hohhot 010110, P.R. China*

Abstract: Apoptosis plays a crucial role in regulating cardiomyopathy and injuries of coxsackievirus B3 (CVB3)-induced viral myocarditis (VM). It has been reported that Astragaloside IV (AST-IV) from *Astragalus membranaceus* could inhibit apoptosis under a variety of pathological conditions *in vivo* or *in vitro*. However, the functional roles of AST-IV in CVB3-induced VM still remain unknown. Here, we found that AST-IV significantly enhanced survival for CVB3-induced mice. AST-IV protected the mice against CVB3-induced virus myocarditis characterized by the increased body weight, decreased serum level of creatine kinase-MB (CK-MB) and lactate dehydrogenase (LDH), supressed expression of Ifn-γ, Il-6 in heart, enhanced systolic and diastolic function of left ventricle. At the pathological level, AST-IV ameliorated the mice against CVB3-induced myocardial damage and myocardial fibrosis. *In vitro*, the results from flow cytometry showed that AST-IV significantly suppressed CVB3-induced cardiomyocytes apoptosis, which also were verified *in vivo*. Moreover, an increased expression of pro-apoptotic genes including FAS, FASL, cleaved caspase-8 and cleaved caspase-3 was found in CVB3-induced cardiomyocytes, while those was inhibited in cardiomyocytes treated with AST-IV. Taken together, the data suggest that AST-IV protected against CVB3-induced myocardial damage and fibrosis, which may partly attribute to supress activation of FAS/FASL signaling pathway.
Key words: apoptosis, astragaloside IV, FAS/FASL signaling pathway, protect effect, virus myocarditis

Introduction

Viral myocarditis (VM) is an important cause of heart failure and sudden death in young, previously healthy individuals [24]. Previous study showed that myocarditis has been estimated to account for up to 12% of sudden cardiac deaths in patients, 40 years of age, and 10% of biopsies from patients with unexplained heart failure had

(Received 1 April 2019 / Accepted 2 June 2019 / Published online in J-STAGE 26 June 2019)
**These authors contributed equally to this work.*
Corresponding authors: X. Liu. e-mail: liulx56@126.com
Y. Dong. e-mail: dongyu010@126.com
Supplementary Figure: refer to J-STAGE: https://www.jstage.jst.go.jp/browse/expanim

Signs of VM [7]. Myocarditis has a wide range of clinical presentation, including asymptomatic electrocardiographic, echocardiographic abnormalities, symptoms of cardiac dysfunction, arrhythmias or heart failure and hemodynamic collapse, which leads to difficulties in diagnosis and classifications [5]. The pathogenesis of VM is still unclear, so evidence-based therapies for VM are currently lacking in clinic [6].

Many studies have revealed that apoptosis played a crucial role in the pathogenesis of cardiac injury in myocarditis. Myocardial apoptosis was induced by either host interferon responses or virus signaling to release progeny at the end of the infectious cycle in acute phase of VM (first 3–4 days after virus infection) [8]. Meanwhile, some cellular signaling pathway associated with apoptosis were activated in heart of CVB3-induced mice, such as FAS/FASL pathway [34], JAK-STAT pathway [3], and mitochondria-dependent pathway[43].Therefore, inhibiting apoptosis was considered a potential therapeutic strategy for viral myocarditis.

Radix astragali as a crucial Chinese herb prescribed for strengthening the constitutions of patients and eliminating toxins from their bodies [41]. Astragaloside IV (AST-IV) as a cycloartane-type triterpene glycoside isolated from Radix astragali has been reported to improve cardiac function [32], inhibit compensatory cardiac hypertrophy and suppress apoptosis [23, 26]. Besides, previous work showed that AST-IV could attenuate myocardial fibrosis by inhibiting TGF-β1 signalling in CVB3-induced cardiomyopathy [5], exerted antiviral effects against CVB3 via up-regulating expression of interferon (Ifn)-γ mRNA[44] and modulated inflammatory response via increasing A20 expression against CVB3-induced virus myocarditis [15]. However, it is not clear whether AST-IV could protect heart form VM via inhibiting CVB3-induced apoptosis.

In the present study, we aimed to investigate the effects of AST-IV from *Astragalus membranaceus* on CVB3-induced myocardial apoptosis. Our study provided evidence to support a novel role of AST-IV in protecting mice against CVB3-induced VM by suppressing the activation of FAS/FASL signal pathway.

Materials and Methods

Experimental animals and coxsackievirus B3

All animal protocols were approved by the Committee of affiliated hospital of Inner Mongolia medical university on Ethics of Animal Experiments (Ethic no. 2015-0108). Animals were treated in accordance with Guide for the Care and Use of Laboratory Animals (8th edition, National Academies Press). Sixty males C57BL/6 mice (8–9 weeks) were purchased from Model Animal Research Center Of Nanjing University (Nanjing, China). All mice were housed in GLP laboratory of Inner Mongolia medical university with a specific pathogen-free environment under a 12 h/12 h light-dark cycle and fed rodent diet *ad libitum*. CVB3 (Nancy strain) was maintained by passage through HeLa cells. HeLa cells was used to perform virus titer assay according to previous report [37]. Virus titer was determined prior to infection by a 50% tissue culture infectious dose ($TCID_{50}$) assay on HeLa cell monolayer. Mice was infected by an intraperitoneal injection with 0.1 ml of PBS containing 10^3 $TCID_{50}$ CVB3.

Inducting VM and experimental protocols

C57BL/6 mice were randomly divided into three groups, namely Blank group (n=20), VM group (CVB3, n=20) and AST-IV treated group (CVB3+ AST-IV, n=20). Purified AST-IV was purchased from Sigma Chemical Co. (St. Louis, MO, USA). Before CVB3 injection, AST-IV treated mice received 100 mg/kg bw of AST-IV (3 ml/30 g bw) per day by gavage to performed a pretreatment [11]. Blank and CVB3-induced mice received 300 μl of saline orally per day. After pretreatment for 2 weeks, mice (CVB3-induced mice and AST-IV treated mice) were induced VM by an intraperitoneal injection with 0.1 ml of PBS containing 10^3 $TCID_{50}$ CVB3[39]. After virus was injected, AST-IV treated mice continuously received 100 mg/kg bw of AST-IV (3 ml/30 g bw) per day by gavage until the end of experiment.

Echocardiography assessment

Echocardiography was used to evaluate cardiac hypertrophy, systolic and diastolic function after virus injection for 3 weeks. A Visual sonics high-resolution Vevo 2100 system (VisualSonics Inc., Toronto, Canada) was used. In brief, mice were anesthetized with 3.0% isoflurane (Airflow velocity: 1 l/min). After the pain reflex disappears and the heart rate stabilized at 400 to 500 beats per min. Parasternal long-axis images were acquired in B-mode with appropriate positioning of the scan head and the maximum LV length identified. The M-mode cursor was positioned perpendicular to the maximum LV dimension in end-diastole and systole, and

M-mode images were obtained for measuring wall thickness and chamber dimensions. Apical four-chamber view was acquired and the peak flow velocities during early diastole (E wave) were measured across the mitral valve. Early-diastolic peak velocity (E' wave) of mitral valve ring was also measured in this view, then E/E' which reflected the left ventricle diastolic function were calculated.

Cell culture, CVB3 stimulation and AST-IV treatment

Primary cardiac myocytes from neonatal mice were prepared as described previously [28]. In brief, the hearts were removed, and the ventricles were minced in calcium- and bicarbonate-free Hanks' buffer with HEPES. These tissue fragments were digested by 0.08% trypsin. The dissociated cells were inoculated in a 10 cm dish for 120 min to enrich the cells according to the differential adherence times of cardiac myocytes and fibroblasts. After cell culture for 120 min, the adherent cells were CFs, and they were cultured continuously in the 10 cm dish with fresh Dulbecco's Modified Eagle Medium (DMEM)/high-glucose with 10% FBS. The cells in suspension were CMs, and they were enriched by centrifugation at 800 rpm for 5 min. After centrifugation, CMs were re-suspended using DMEM/high-glucose with 10% FBS and 0.1 mmol/l bromodeoxyuridine and then were inoculated in a 12- or 6-well plate at 2,000 cells/cm^2. The cells were maintained in an incubator at 37°C in the presence of 5% CO_2.

CMs were randomly assigned to one of three experimental groups as follows: (1) Blank; (2) CVB3: infection with CVB3 at multiplicities of infection (MOI)=1[4]; (3) CVB3+ AST-IV: infection with CVB3 at MOI=1 and treatment with 250 μg/ml AST-IV [38]. At the beginning of the experiment, the CVB3+ AST-IV groups of myocytes were pre-treated with 250 μg/ml AST-IV for 2 h, while the Blank and OA groups were pretreated with FBS-free DMEM/high-glucose for 2 h. After pretreated with AST-IV, the CVB3 groups and CVB3+ AST-IV groups were infection with CVB3 at MOI=1, and Blank group was cultured with fresh DMEM/high-glucose medium. The cells were exposed to those drugs throughout the experimental period.

Primary cardiomyocytes apoptosis array by flow cytometry

Apoptosis of Primary cardiomyocytes (CMs) was examined by detecting phosphatidylserine exposure on cell membrane with Annexin V as described. Briefly, CMs were seeded into 6-well plates and stimulated according to the methods mentioned above for 48 h. The medium was collected, and CMs were digested by trypsin. After mixing medium and digested CMs, the cell suspension was centrifugated in 1,000 g for 5 min. The cells were washed twice with cold phosphate-buffered saline (pH 7.4) and were stained with Annexin V-FITC (25 ng/ml; green fluorescence) and dye exclusion (PI, red fluorescence) according to protocol provided by Annexin V-FITC Apoptosis Detection Kit I (BD bioscience, San Diego, CA, USA). After staining, apoptosis of CMs was analyzed with flow cytometry.

Histological analysis

After CVB3 infection for 3 weeks, mice were anesthetized with 3.0% isoflurane and heart was arrested with a 10% potassium chloride solution at end-diastole and then fixed in 4% paraformaldehyde. Fixed hearts were embedded in paraffin and cut transversely into 5 μm sections. Serial heart sections were stained with hematoxylin and eosin (H&E) to measure cardiac damage [1]. The degree of collagen deposition was detected by picrosirius red (PSR) staining, and images were analyzed using a quantitative digital image analysis system (Image-Pro Plus 6.0).

Western blotting and quantitative real-time PCR

Protein were extracted with radioimmunprecipitation assay (RIPA) buffer (50 mM Tris-HCl pH 7.4, 150 mM NaCl, 1mM EDTA, 0.25% sodium deoxycholate, 0.1% SDS and protease inhibitor cocktail). Homogenates were sonicated and centrifuged at 4°C for 15 min, and the supernatants were used for western blotting. 20–50 μg of protein were separated by SDS-PAGE and transferred to a NC membrane (Millipore, Bedford, MA, USA). After being blocked with 5% non-fat milk, the membranes were incubated with the following primary antibodies overnight at 4°C: anti-mouse FAS, anti-mouse FASL, anti-mouse caspase-8, anti-mouse caspase-3 and anti-GAPDH (Cell Signaling Technology, Danvers, MA, USA). Subsequently, the membrane was incubated with a horseradish peroxidase-conjugated secondary antibody (Santa Cruz Biotechnology, Santa Cruz, CA, USA), and exposed to ECL reagent for detection of protein expression. Total RNA was extracted using TRIzol reagent (Invitrogen, Grand Island, NY, USA), and first-stand cDNA was synthesized using reverse transcriptase (Ta-

kara, Kusatsu, Japan). Real-time PCR with SYBR Green (Takara) was performed to examine the relative mRNA levels of indicated genes. The primer was showed as following, Ifn-γ: Forward Primer: GCCACGGCACAGTCATTGA, Reverse Primer: TGCTGATGGCCTGATTGTCTT; Il-6: Forward Primer: CTGCAAGAGACTTCCATCCAG, Reverse Primer: AGTGGTATAGACAGGTCTGTTGG. CVB3 copy number in mouse heart was detected by RT-PCR, Forward Primer:5'-CCCTGAATGCGGCTAATCC-3', Reverse Primer: 5'-ATTGTCACCATAAGC AGCCA-3'.

Terminal deoxynucleotidyl transferase dUTP nick end labeling (TUNEL) staining

The TUNEL assay was performed using the *In Situ* Cell Death Detection kit (Roche, Basel, Switzerland) as previously described [9].

Biochemical assay

After CVB3 infection for 3 weeks, mice were anesthetized with 3.0% isoflurane and collecting peripheral blood by retro-orbital blood collection. Peripheral blood was centrifuged with 8,000 × g for 15 min to collecting serum. Serum LDH and CK-MB level was detected with LDH Assay Kit / Lactate Dehydrogenase Assay Kit (Abcam, Cambridge, MA, USA) and Mouse Creatine Kinase MB isoenzyme, CK-MB ELISA Kit (Sangon Biotech, Shanghai, China), respectively.

Statistical analysis

Data were presented as mean ± SEM. Differences among all groups were assessed using a one-way analysis of variance (ANOVA) followed by the Newman-Keuls post hoc test. A *P*-value less than 0.05 was considered statistically significant.

Results

AST-IV treatment ameliorated CVB3-induced virus myocarditis

We firstly examined the effect of AST-IV on CVB3-induced VM model in mice, the chemical structure of

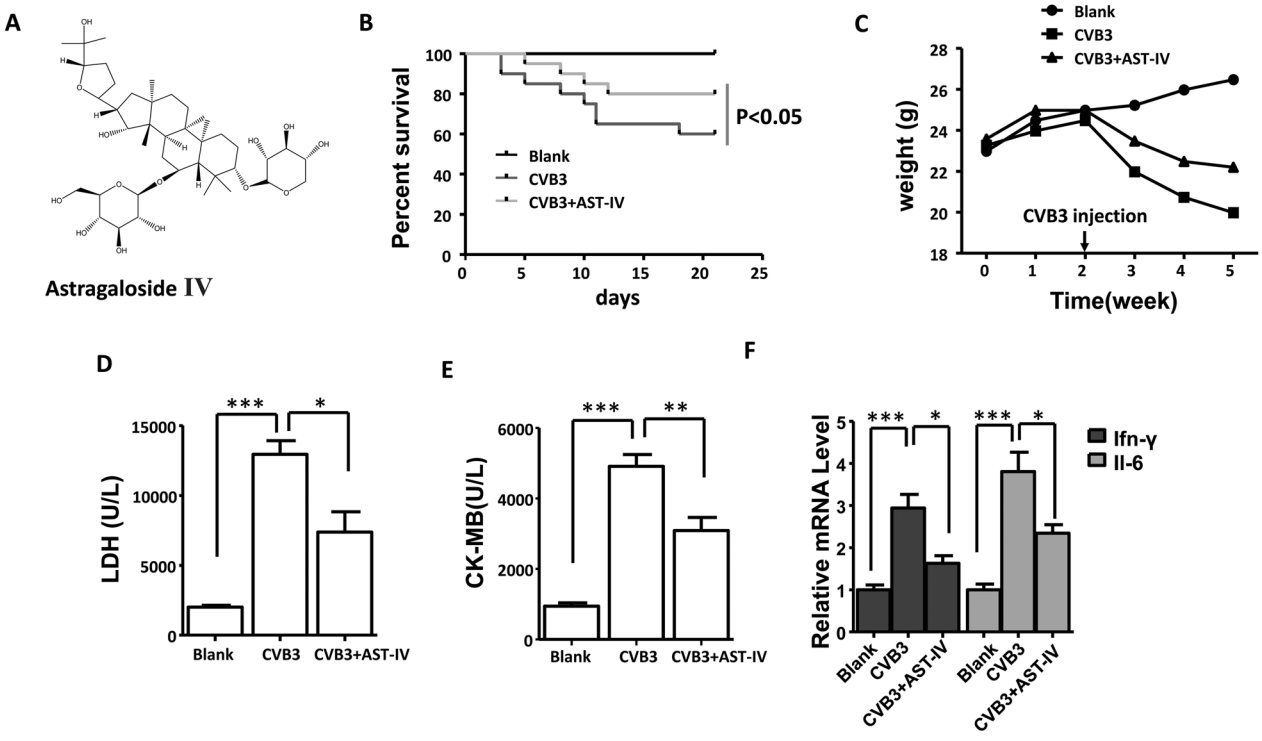

Fig. 1. Astragaloside IV (AST-IV) ameliorated coxsackievirus B3 (CVB3)-induced virus myocarditis. (A) The chemical structure of AST-IV. (B) Survival of mice was monitored within 3 weeks post infection (n=20 per group). (C) The body weight change of mice was monitored within 3 weeks post infection (n=20 per group). The serum levels of creatine kinase-MB (CK-MB) (D, n=5 per group) and lactate dehydrogenase (LDH) (E, n=5 per group). (F) The mRNA level of IFN-γ and Il-6 in heart (n=5 per group). The data were calculated with GraphPad Prism and presented as mean ± SEM, ***P*<0.05, ***P*<0.01 and ****P*<0.001.

AST-IV was showed in Fig. 1A. Survival curve showed enhanced mortality in CVB3-induced mice (death: 8 mice, n=20) compared to Blanks mice (death: 0 mice, n=20) from CVB3 injection to experimental end, while mortality rate was significantly inhibited in AST-IV treated mice (death: 4 mice, n=20, Fig. 1B). Compared to Blank mice, VM mice a dramatic and continuous loss of bodyweight as maximal to 23.1%, while AST-IV treated mice had a little fluctuation in bodyweight (Fig. 1C). Furthermore, the increased level of CK-MB and LDH in serum induced by CVB3 infection showed a significant reduction in AST-IV treated mice (Figs. 1D and E). In addition, a significantly increased expression of Ifn-γ and Il-6 was found in heart of CVB3-induced mice compared to Blank mice, while those was significantly supressed in heart of AST-IV treated mice compared (Fig. 1F). These results indicate that AST-IV treatment dramatically alleviated CVB3-induced inflammation reaction and cardiac damage. Moreover, no significant difference for CVB3 RNA copy number was found in heart after CVB3 injection for 3 weeks between CVB3-induced mice and AST-IV treated mice, which indicated that the protective effect of AST-IV on CVB3-induced VM was not associated with its anti-viral effect (Supplementary Fig. 1).

AST-IV treatment ameliorated CVB3-induced cardiac systolic and diastolic function changes

To study the role of AST-IV on the cardiac systolic and diastolic function, Cardiac function was measured by echocardiography after virus injection for 3 weeks. Ultrasonic results show the overall echo of the heart is attenuated in heart of CVB3-induced mice, while cardiac function was improved in heart of AST-IV treated mice (Fig. 2A). Compared to Blank mice, we found that a significantly impaired left ventricle (LV) function, as indexed by increased Left ventricle end diastolic posterior wall dimension (LVPWd, 1.30 ± 0.15 versus 0.77 ± 0.049, $P<0.001$), decreased ejection fraction (EF%) (42.1 ± 7.06% versus 56.50 ± 6.65, $P<0.01$) and increased E/E' (42.50 ± 6.67 versus 19.10 ± 5.06, $P<0.001$) in heart of CVB3-induced mice, while heart of AST-IV treated mice exhibited a better cardiac function than CVB3-induced heart (LVPWd, 1.033 ± 0.20 versus 1.30 ± 0.15, $P=0.026$; EF%, 48.30 ± 4.39% versus 56.50 ± 6.65%, $P=0.03$, E/E'; 48.30 ± 4.39 versus 56.50 ± 6.65, $P=0.03$; E/E', 28.10 ± 7.98 versus 42.1 ± 7.06%, $P<0.001$) (Figs. 2B–D). Together, these data show that AST-IV treatment attenuated CVB3-induced cardiac dysfunction.

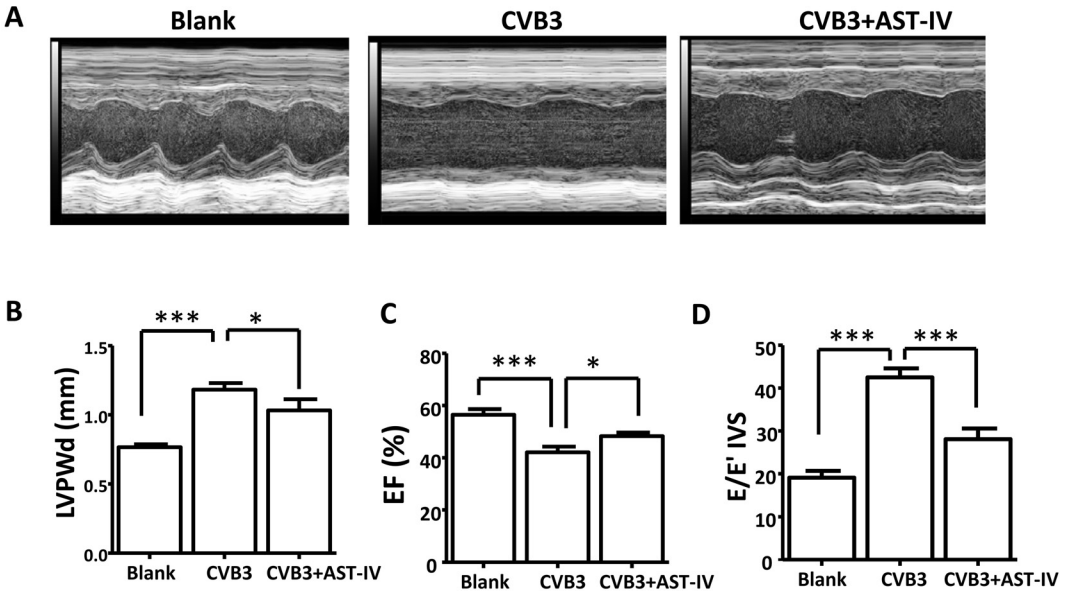

Fig. 2. Astragaloside IV (AST-IV) ameliorated coxsackievirus B3 (CVB3)-induced cardiac systolic and diastolic function changes. (A) Representative M-mode echocardiographic tracings of different groups. (B–D) Cardiac function was assessed by Left ventricle end diastolic posterior wall dimension (LVPWd) (B, n=10 per group), EF% (n=10 per group) and E/E' (n=10 per group). The data were calculated with GraphPad Prism and presented as mean ± SEM, *$P<0.05$, **$P<0.01$ and ***$P<0.001$.

AST-IV treatment protected mouse heart against CVB3-induced cardiac damage and fibrosis

To advanced illustrate the role of AST-IV on CVB3-induced virus myocarditis, histological analysis of heart sections was performed to examine degree of cardiac damage and fibrosis. H&E staining of heart sections showed that the area of cardiac necrosis was significantly aggravated in heart of CVB3-induced mice comparing to Blank mice after CVB3 injection for 3 weeks, while the degree of cardiac necrosis was significantly attenuated in heart of AST-IV treated mice (Fig. 3A). The degree of collagen deposition in heart was detected by picrosirius red (PSR) staining. Compared with Blank mice, a significantly increased cardiac fibrosis was found in heart of VM mice, while cardiac fibrosis level was ameliorated in heart of AST-IV treated mice (Fig. 3B). These results demonstrated that AST-IV treatment had significantly effect on CVB3-induced cardiac necrosis and fibrosis.

AST-IV treatment inhibited CVB3-induced apoptosis

Apoptosis played an important role on occurrence of dilated cardiomyopathy after VM [33]. We speculated that the protective effect of AST-IV treatment on CMs activity was associated with inhibiting myocardial apoptosis. To verify our hypothesis, TUNEL staining of heart section *in vivo* was performed. An increased apoptosis level was found in heart of CVB3-induced mice compared to Blank mice, while apoptosis level was inhibited in heart of AST-IV treated mice compared to CVB3-induced mice (Fig. 4A). The same result was confirmed by CMs apoptosis array by flow cytometry *in vitro*. The result showed that 2.7% of early apoptosis, 40.2% of late apoptosis and 4.9% of necrosis were found in CVB3-induced CMs after CVB3 infection for 48 h, while those were 1.3%, 1.4% and 0.6% in AST-IV treated CMs, respectively (Fig. 4B).

Numerous studies have demonstrated that FAS/FASL signal pathway had closely relationship with apoptosis [36]. Therefore, we investigated the protein levels of FAS, FASL, cleaved caspase-8 and cleaved caspase-3 level by western blotting *in vitro*. After CMs were induced by CVB3 and treated with AST-IV for 48 h, a significant increased expression of FAS, FASL, cleaved

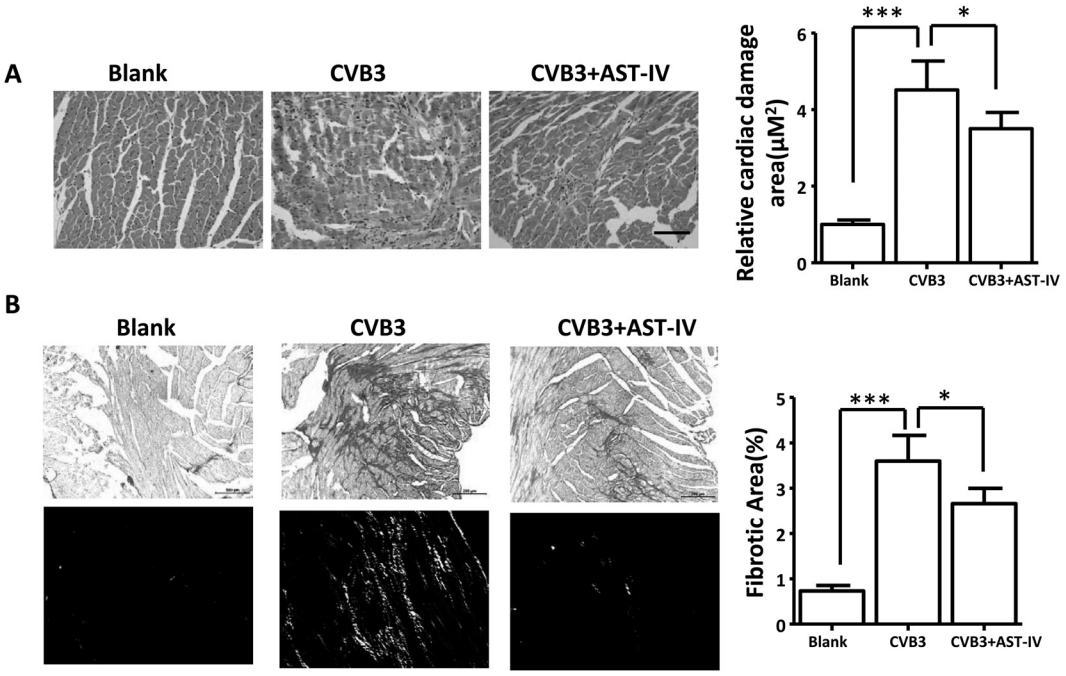

Fig. 3. Astragaloside IV (AST-IV) protected mice heart from coxsackievirus B3 (CVB3)-induced cardiac damage and fibrosis. (A) H&E staining of heart sections and quantitative data (scale bars:100 μM, n=6 per group). (B) Picrosirius red-stained transverse sections of the left ventricle from the indicated groups and quantitative data (Scale bars:200 μM, n=6 per group. Upper: image under bright field, lower: image under Polarized light). The data were calculated with GraphPad Prism and presented as mean ± SEM, **P*<0.05, ***P*<0.01 and ****P*<0.001.

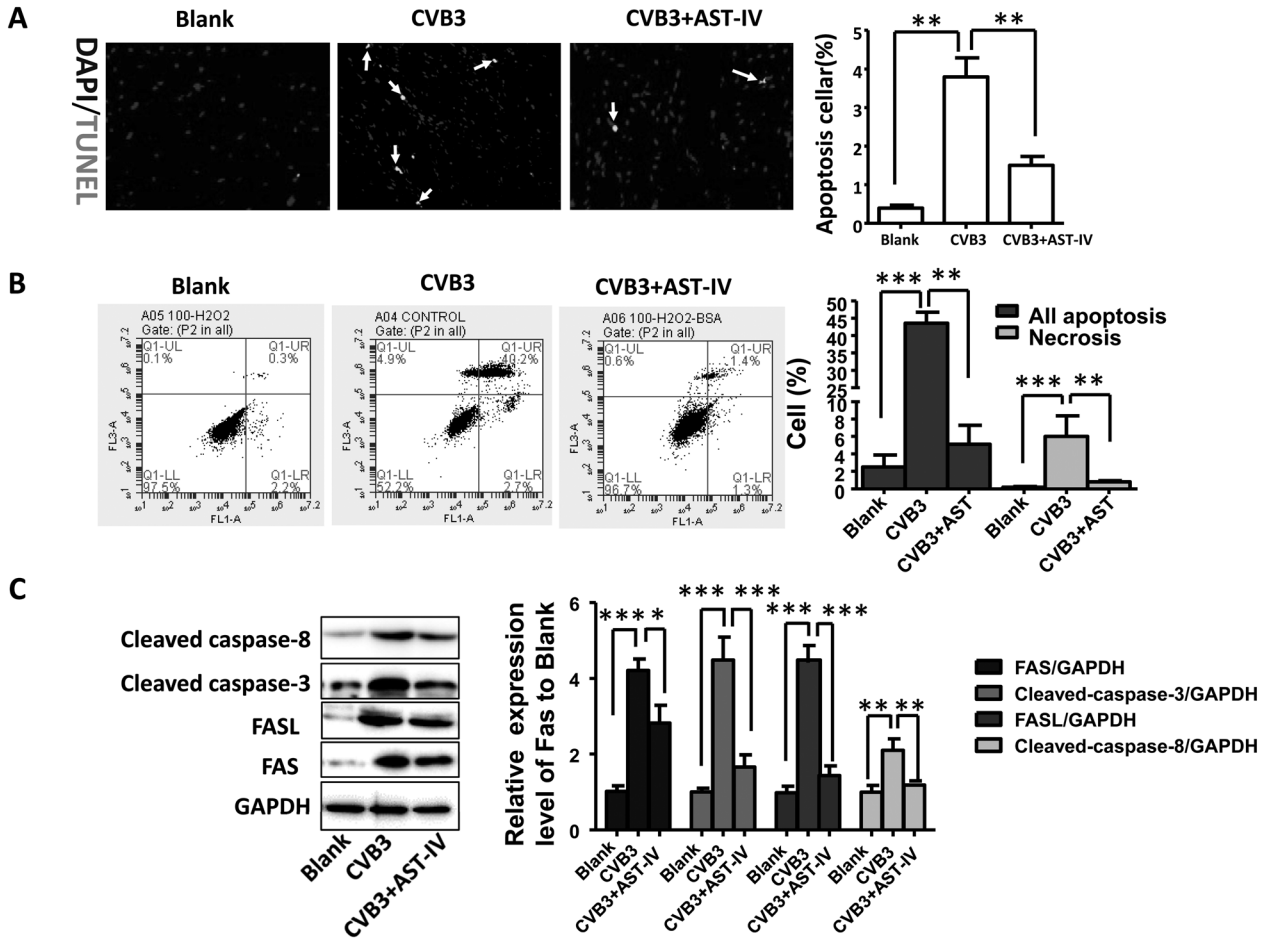

Fig. 4. Astragaloside IV (AST-IV) treatment attenuated coxsackievirus B3 (CVB3)-induced apoptosis *in vivo and in vitro*. (A) Terminal deoxynucleotidyl transferase dUTP nick end labeling (TUNEL) staining results of heart sections and quantitative data (n=6 per group); (B) Cardiac myocytes apoptosis was detected by flow cytometer; (C) Expression level of FAS, FASL, caspase-8 and caspase-3 *in vitro* was detected by western blot and quantitative data (n=3 per group). The data were calculated with GraphPad Prism and presented as mean ± SEM, **P*<0.05, ***P*<0.01 and ****P*<0.001.

caspase-8 and cleaved caspase-3 were found in CVB3-induced CMs comparing to Blank CMs, while expression level of those protein was significantly inhibited in AST-IV treated CMs (Fig. 4C). In summary, our data implicated that AST-IV treatment could protect heart from CVB3-induced apoptosis via regulating FAS/FASL signal pathway

Discussion

Our current study demonstrated, the beneficial effect of AST-IV on CVB3-induced VM and protected mice from CVB3-induced cardiac dysfunction, cardiac damage and chronic fibrosis. Our results showed suppressing the activation of FAS/FASL signal pathway as a protective mechanism of AST-IV to prevent CVB3-induced apoptosis.

Apoptosis played an important role on CVB3-induced VM. In the acute phase of VM (virus infection for 3–4 days), direct proteolytic damage was induced for virus replication and interaction with myocyte signaling, and recognition of viral pathogen motifs through cardiac Toll-like receptors [2, 25]. Meanwhile, cardiac resident cells released a lot of proinflammation cytokines, including g interleukin-1β (IL1β), Il-6, IL-18, tumor necrosis factor-α (TNF-α), and type I and type II interferons (IFNs) [14]. Among cytokines, Type I interferons (IFN-α and IFN-β) had a range of effects on infected cells, including inducing cardiomyocyte apoptosis via stimulating p53-mediated apoptosis signal [12]. Besides, in

chronic phase of VM (>14 days after virus infection), regulatory T cells and alternatively activated (M2) macrophages released a range of anti-inflammation cytokines to resolute the immune response and replace dead tissue with a fibrotic scar, including TGF-β and IL-10 [31]. Those anti-inflammation cytokines also could induce cardiomyocyte apoptosis via FAS/FASL pathway [13, 30]. In our study, AST-IV treatment could significantly inhabit CVB3-induced cardiomyocyte apoptosis, which interpreted the mechanism of the protective effect of AST-IV on CVB3-induced VM.

The FAS/FASL system played a significant role in multiple causes-induced cardiomyocyte apoptosis. A significantly up-regulated FAS expression was found in pathological process of CVB3 [18], ischemia-reperfusion injury [22] and transplant rejection [27] -induced cardiomyocyte apoptosis, which was consistent with our findings. Different from our results, Zhang *et al.* found that the expression level of FASL was not enhanced in heart of CVB3-induced mice [45]. The reason for this difference could be attributed to inconsistency between cardiomyocytes and myocardial tissue. The mechanism of CVB3-induced FASL expression in cardiomyocytes was unclear. However, Dai *et al.* found that CVB3 replication could activate c-Jun N-Terminal Kinase (JNK) and p38 MAPK *in vitro* [10], while activation of JNK could enhance FAS/FASL expression via c-Jun [17]. Meanwhile, a significantly up-regulated FASL expression was also found in ischemia/reperfusion-induced cardiomyocytes apoptosis *in vitro* [20].

The previous study showed that caspase-3 had critical role in multiple pathological factors-induced cardiomyocyte apoptosis [29]. There are at least 2 pathways were involved in capase-3 activation of human heart, mitochondria disruption mediated apoptosis pathway and FAS receptor-mediated death receptor pathway. Different from the mitochondria disruption mediated apoptosis pathway, FAS receptor-mediated death receptor pathway involved activation of caspase-8 [35]. Activated caspase-8 led to caspase-3 activation. Activated caspase-3 then cleaves a substrate such as poly-(ADP-ribose) polymerase, leading to DNA fragmentation and apoptosis. In our study, after CMs was induced by CVB3 for 48h, a significant increased expression of FAS, FASL, caspase-3 and caspase-8 was found comparing to Blank CMs, while those were inhibited in CMs of AST-IV treatment. Therefore, our results demonstrated that AST-IV could inhabit CVB3-induced apoptosis via supressed activation of FAS/FASL pathway.

Astragalus membranaceus was widely used in traditional Chinese medicine as an antiperspirant, antihypertensive, diuretic, and tonic treatments [40]. Previous study showed that *Astragalus membranaceus* and its extracts could protect heart from Ischemia/reperfusion injury [21], oxidative stress [19, 26], and modulate immune reaction and cardiac energy metabolism [16]. It had been reported that AST-IV could protect heart from CVB3-induced VM via modulating inflammatory response [15]. Besides, AST-IV could inhibit multiple pathological factors-induced cardiomyocytes apoptosis, such as oxidative stress [26], ischemia/reperfusion injury [42]. However, it was not been reported whether AST-IV could protect heart from VM via inhibiting CVB3-induced cardiomyocytes apoptosis. In our study, a significantly protective effect of AST-IV on VM was found, which had close association with inhibiting myocardial apoptosis via supressing activation of FAS/FASL pathway.

Acknowledgments

The study was supported by National Natural Science Foundation of China (81460066 to Xiaolei LIU).

References

1. Althof, N., Goetzke, C.C., Kespohl, M., Voss, K., Heuser, A., Pinkert, S., Kaya, Z., Klingel, K. and Beling, A. 2018. The immunoproteasome-specific inhibitor ONX 0914 reverses susceptibility to acute viral myocarditis. *EMBO Mol. Med.* 10: 200–218. [Medline] [CrossRef]
2. Badorff, C., Lee, G.H., Lamphear, B.J., Martone, M.E., Campbell, K.P., Rhoads, R.E. and Knowlton, K.U. 1999. Enteroviral protease 2A cleaves dystrophin: evidence of cytoskeletal disruption in an acquired cardiomyopathy. *Nat. Med.* 5: 320–326. [Medline] [CrossRef]
3. Barry, S.P., Townsend, P.A., Latchman, D.S. and Stephanou, A. 2007. Role of the JAK-STAT pathway in myocardial injury. *Trends Mol. Med.* 13: 82–89. [Medline] [CrossRef]
4. Belkaya, S., Kontorovich, A.R., Byun, M., Mulero-Navarro, S., Bajolle, F., Cobat, A., Josowitz, R., Itan, Y., Quint, R., Lorenzo, L., Boucherit, S., Stoven, C., Di Filippo, S., Abel, L., Zhang, S.Y., Bonnet, D., Gelb, B.D. and Casanova, J.L. 2017. Autosomal Recessive Cardiomyopathy Presenting as Acute Myocarditis. *J. Am. Coll. Cardiol.* 69: 1653–1665. [Medline] [CrossRef]
5. Chen, P., Xie, Y., Shen, E., Li, G.G., Yu, Y., Zhang, C.B., Yang, Y., Zou, Y., Ge, J., Chen, R. and Chen, H. 2011. Astragaloside IV attenuates myocardial fibrosis by inhibiting TGF-β1 signaling in coxsackievirus B3-induced cardiomy-

opathy. *Eur. J. Pharmacol.* 658: 168–174. [Medline] [CrossRef]
6. Cooper, L.T. Jr. 2009. Myocarditis. *N. Engl. J. Med.* 360: 1526–1538. [Medline] [CrossRef]
7. Corsten, M.F., Heggermont, W., Papageorgiou, A.P., Deckx, S., Tijsma, A., Verhesen, W., van Leeuwen, R., Carai, P., Thibaut, H.J., Custers, K., Summer, G., Hazebroek, M., Verheyen, F., Neyts, J., Schroen, B. and Heymans, S. 2015. The microRNA-221/-222 cluster balances the antiviral and inflammatory response in viral myocarditis. *Eur. Heart J.* 36: 2909–2919. [Medline] [CrossRef]
8. Corsten, M.F., Schroen, B. and Heymans, S. 2012. Inflammation in viral myocarditis: friend or foe? *Trends Mol. Med.* 18: 426–437. [Medline] [CrossRef]
9. Crowley, L.C., Marfell, B.J. and Waterhouse, N.J. 2016. Detection of DNA fragmentation in apoptotic cells by TUNEL. *Cold Spring Harb. Protoc.* 2016: pdb.prot087221. [Medline] [CrossRef]
10. Dai, Q., Zhang, D., Yu, H., Xie, W., Xin, R., Wang, L., Xu, X., He, X., Xiong, J., Sheng, H., Zhang, L., Zhang, K. and Hu, X. 2017. Berberine Restricts Coxsackievirus B Type 3 Replication via Inhibition of c-Jun N-Terminal Kinase (JNK) and p38 MAPK Activation In Vitro. *Med. Sci. Monit.* 23: 1448–1455. [Medline] [CrossRef]
11. Du, Q., Zhang, S., Li, A., Mohammad, I.S., Liu, B. and Li, Y. 2018. Astragaloside IV Inhibits Adipose Lipolysis and Reduces Hepatic Glucose Production *via* Akt Dependent PDE3B Expression in HFD-Fed Mice. *Front. Physiol.* 9: 15. [Medline] [CrossRef]
12. Esfandiarei, M., and McManus, B.M. 2008. Molecular biology and pathogenesis of viral myocarditis. *Annu. Rev. Pathol.* 3: 127–155. [Medline] [CrossRef]
13. Furukawa, H., Oshima, K., Tung, T., Cui, G., Laks, H. and Sen, L. 2008. Overexpressed exogenous IL-4 And IL-10 paradoxically regulate allogenic T-cell and cardiac myocytes apoptosis through FAS/FASL pathway. *Transplantation* 85: 437–446. [Medline] [CrossRef]
14. Fuse, K., Chan, G., Liu, Y., Gudgeon, P., Husain, M., Chen, M., Yeh, W.C., Akira, S. and Liu, P.P. 2005. Myeloid differentiation factor-88 plays a crucial role in the pathogenesis of Coxsackievirus B3-induced myocarditis and influences type I interferon production. *Circulation* 112: 2276–2285. [Medline] [CrossRef]
15. Gui, J., Chen, R., Xu, W. and Xiong, S. 2015. Remission of CVB3-induced myocarditis with Astragaloside IV treatment requires A20 (TNFAIP3) up-regulation. *J. Cell. Mol. Med.* 19: 850–864. [Medline] [CrossRef]
16. Han, J.Y., Li, Q., Ma, Z.Z. and Fan, J.Y. 2017. Effects and mechanisms of compound Chinese medicine and major ingredients on microcirculatory dysfunction and organ injury induced by ischemia/reperfusion. *Pharmacol. Ther.* 177: 146–173. [Medline] [CrossRef]
17. He, P., Zhang, B., Liu, D., Bian, X., Li, D., Wang, Y., Sun, G. and Zhou, G. 2016. Hepatitis B Virus X Protein Modulates Apoptosis in NRK-52E Cells and Activates Fas/FasL Through the MLK3-MKK7-JNK3 Signaling Pathway. *Cell. Physiol. Biochem.* 39: 1433–1443. [Medline] [CrossRef]
18. Huang, T.F., Wu, X.H., Wang, X. and Lu, I.J. 2016. Fas-FasL expression and myocardial cell apoptosis in patients with viral myocarditis. *Genet. Mol. Res.* 15: gmr7607. [Medline] [CrossRef]
19. Huang, Y.F., Lu, L., Zhu, D.J., Wang, M., Yin, Y., Chen, D.X. and Wei, L.B. 2016. Effects of *Astragalus* Polysaccharides on Dysfunction of Mitochondrial Dynamics Induced by Oxidative Stress. *Oxid. Med. Cell. Longev.* 2016: 9573291. [Medline] [CrossRef]
20. Jiang, C.M., Han, L.P., Li, H.Z., Qu, Y.B., Zhang, Z.R., Wang, R., Xu, C.Q. and Li, W.M. 2008. Calcium-sensing receptors induce apoptosis in cultured neonatal rat ventricular cardiomyocytes during simulated ischemia/reperfusion. *Cell Biol. Int.* 32: 792–800. [Medline] [CrossRef]
21. Jin, Y., Chen, Q., Li, X., Fan, X. and Li, Z. 2014. Astragali Radix protects myocardium from ischemia injury by modulating energy metabolism. *Int. J. Cardiol.* 176: 1312–1315. [Medline] [CrossRef]
22. Liu, X.M., Yang, Z.M. and Liu, X.K. 2017. Fas/FasL induces myocardial cell apoptosis in myocardial ischemia-reperfusion rat model. *Eur. Rev. Med. Pharmacol. Sci.* 21: 2913–2918. [Medline]
23. Liu, Z.H., Liu, H.B. and Wang, J. 2018. Astragaloside IV protects against the pathological cardiac hypertrophy in mice. *Biomed. Pharmacother.* 97: 1468–1478. [Medline] [CrossRef]
24. Mahfoud, F., Gärtner, B., Kindermann, M., Ukena, C., Gadomski, K., Klingel, K., Kandolf, R., Böhm, M. and Kindermann, I. 2011. Virus serology in patients with suspected myocarditis: utility or futility? *Eur. Heart J.* 32: 897–903. [Medline] [CrossRef]
25. Mann, D.L. 2011. The emerging role of innate immunity in the heart and vascular system: for whom the cell tolls. *Circ. Res.* 108: 1133–1145. [Medline] [CrossRef]
26. Mei, M., Tang, F., Lu, M., He, X., Wang, H., Hou, X., Hu, J., Xu, C. and Han, R. 2015. Astragaloside IV attenuates apoptosis of hypertrophic cardiomyocyte through inhibiting oxidative stress and calpain-1 activation. *Environ. Toxicol. Pharmacol.* 40: 764–773. [Medline] [CrossRef]
27. Miller, L.W., Granville, D.J., Narula, J. and McManus, B.M. 2001. Apoptosis in cardiac transplant rejection. *Cardiol. Clin.* 19: 141–154. [Medline] [CrossRef]
28. Mohamed, B.A., Barakat, A.Z., Zimmermann, W.H., Bittner, R.E., Mühlfeld, C., Hünlich, M., Engel, W., Maier, L.S. and Adham, I.M. 2012. Targeted disruption of Hspa4 gene leads to cardiac hypertrophy and fibrosis. *J. Mol. Cell. Cardiol.* 53: 459–468. [Medline] [CrossRef]
29. Narula, J., Pandey, P., Arbustini, E., Haider, N., Narula, N., Kolodgie, F.D., Dal Bello, B., Semigran, M.J., Bielsa-Masdeu, A., Dec, G.W., Israels, S., Ballester, M., Virmani, R., Saxena, S. and Kharbanda, S. 1999. Apoptosis in heart failure: release of cytochrome c from mitochondria and activation of caspase-3 in human cardiomyopathy. *Proc. Natl. Acad. Sci. USA* 96: 8144–8149. [Medline] [CrossRef]
30. Okada, H., Takemura, G., Kosai, K., Li, Y., Takahashi, T., Esaki, M., Yuge, K., Miyata, S., Maruyama, R., Mikami, A., Minatoguchi, S., Fujiwara, T. and Fujiwara, H. 2005. Postinfarction gene therapy against transforming growth factor-beta signal modulates infarct tissue dynamics and attenuates

left ventricular remodeling and heart failure. *Circulation* 111: 2430–2437. [Medline] [CrossRef]
31. Papageorgiou, A.P., and Heymans, S. 2012. Interactions between the extracellular matrix and inflammation during viral myocarditis. *Immunobiology* 217: 503–510. [Medline] [CrossRef]
32. Qiu, X., Guo, Q., Xiong, W., Yang, X. and Tang, Y.Q. 2016. Therapeutic effect of astragaloside-IV on bradycardia is involved in up-regulating klotho expression. *Life Sci.* 144: 94–102. [Medline] [CrossRef]
33. Roman, R.J. 2002. P-450 metabolites of arachidonic acid in the control of cardiovascular function. *Physiol. Rev.* 82: 131–185. [Medline] [CrossRef]
34. Seko, Y., Kayagaki, N., Seino, K., Yagita, H., Okumura, K. and Nagai, R. 2002. Role of Fas/FasL pathway in the activation of infiltrating cells in murine acute myocarditis caused by Coxsackievirus B3. *J. Am. Coll. Cardiol.* 39: 1399–1403. [Medline] [CrossRef]
35. Tanaka, M., Mokhtari, G.K., Terry, R.D., Balsam, L.B., Lee, K.H., Kofidis, T., Tsao, P.S. and Robbins, R.C. 2004. Overexpression of human copper/zinc superoxide dismutase (SOD1) suppresses ischemia-reperfusion injury and subsequent development of graft coronary artery disease in murine cardiac grafts. *Circulation* 110:(Suppl 1): II200–II206. [Medline] [CrossRef]
36. van Empel, V.P., Bertrand, A.T., Hofstra, L., Crijns, H.J., Doevendans, P.A. and De Windt, L.J. 2005. Myocyte apoptosis in heart failure. *Cardiovasc. Res.* 67: 21–29. [Medline] [CrossRef]
37. Van Linthout, S., Savvatis, K., Miteva, K., Peng, J., Ringe, J., Warstat, K., Schmidt-Lucke, C., Sittinger, M., Schultheiss, H.P. and Tschöpe, C. 2011. Mesenchymal stem cells improve murine acute coxsackievirus B3-induced myocarditis. *Eur. Heart J.* 32: 2168–2178. [Medline] [CrossRef]
38. Wang, X., Wang, Y., Hu, J.P., Yu, S., Li, B.K., Cui, Y., Ren, L. and Zhang, L.D. 2017. Astragaloside IV, a Natural PPARγ Agonist, Reduces Aβ Production in Alzheimer's Disease Through Inhibition of BACE1. *Mol. Neurobiol.* 54: 2939–2949. [Medline] [CrossRef]
39. Wang, Y., Jia, L., Shen, J., Wang, Y., Fu, Z., Su, S.A., Cai, Z., Wang, J.A. and Xiang, M. 2018. Cathepsin B aggravates coxsackievirus B3-induced myocarditis through activating the inflammasome and promoting pyroptosis. *PLoS Pathog.* 14: e1006872. [Medline] [CrossRef]
40. Wang, Y., Li, J., Xuan, L., Liu, Y., Shao, L., Ge, H., Gu, J., Wei, C. and Zhao, M. 2018. *Astragalus* Root dry extract restores connexin43 expression by targeting miR-1 in viral myocarditis. *Phytomedicine* 46: 32–38. [Medline] [CrossRef]
41. Wang, Z.F., Ma, D.G., Zhu, Z., Mu, Y.P., Yang, Y.Y., Feng, L., Yang, H., Liang, J.Q., Liu, Y.Y., Liu, L. and Lu, H.W. 2017. Astragaloside IV inhibits pathological functions of gastric cancer-associated fibroblasts. *World J. Gastroenterol.* 23: 8512–8525. [Medline] [CrossRef]
42. Yin, B., Hou, X.W. and Lu, M.L. 2019. Astragaloside IV attenuates myocardial ischemia/reperfusion injury in rats via inhibition of calcium-sensing receptor-mediated apoptotic signaling pathways. *Acta Pharmacol. Sin.* 40: 599-607. [Medline]
43. Zhang, H.M., Yanagawa, B., Cheung, P., Luo, H., Yuan, J., Chau, D., Wang, A., Bohunek, L., Wilson, J.E., McManus, B.M. and Yang, D. 2002. Nip21 gene expression reduces coxsackievirus B3 replication by promoting apoptotic cell death via a mitochondria-dependent pathway. *Circ. Res.* 90: 1251–1258. [Medline] [CrossRef]
44. Zhang, Y., Zhu, H., Huang, C., Cui, X., Gao, Y., Huang, Y., Gong, W., Zhao, Y. and Guo, S. 2006. Astragaloside IV exerts antiviral effects against coxsackievirus B3 by upregulating interferon-gamma. *J. Cardiovasc. Pharmacol.* 47: 190–195. [Medline] [CrossRef]
45. Zhang, Z.C., Li, S.J., Yang, Y.Z., Chen, R.Z., Ge, J.B. and Chen, H.Z. 2007. Effect of astragaloside on cardiomyocyte apoptosis in murine coxsackievirus B3 myocarditis. *J. Asian Nat. Prod. Res.* 9: 145–151. [Medline] [CrossRef]